Two-dimensional transport and transfer of a single atomic qubit in optical tweezers

J. Beugnon, C. Tuchendler, H. Marion, A. Gaëtan, Y. Miroshnychenko,
Y.R.P. Sortais, A.M. Lance M.P.A. Jones, G. Messin, A. Browaeys, P. Grangier

Laboratoire Charles Fabry de l'Institut d'Optique, CNRS, Univ. Paris-sud,
Campus Polytechnique, RD 128, 91127 Palaiseau cedex, France
(Dated: February 1, 2008)

Quantum computers have the capability of out-performing their classical counterparts for certain computational problems [1]. Several scalable quantum computing architectures have been proposed. An attractive architecture is a large set of physically independant qubits, arranged in three spatial regions where (i) the initialized qubits are stored in a register, (ii) two qubits are brought together to realize a gate, and (iii) the readout of the qubits is performed [2, 3]. For a neutral atom-based architecture, a natural way to connect these regions is to use optical tweezers to move qubits within the system. In this letter we demonstrate the coherent transport of a qubit, encoded on an atom trapped in a sub-micron tweezer, over a distance typical of the separation between atoms in an array of optical traps [4, 5, 6]. Furthermore, we transfer a qubit between two tweezers, and show that this manipulation also preserves the coherence of the qubit.

In the quest for an implementation of a quantum computer, scalability is a major concern. In the trapped ion approach (see e.g. [7]), a lot of effort is being devoted to building arrays of small ion traps [8], and to moving ion qubits whilst avoiding heating and decoherence [9]. Neutral atoms also offer promising properties for the realization of large quantum registers. For example, one- or two-dimensional adressable arrays of dipole traps have been demonstrated using holographic techniques [4], micro-fabricated elements [5], or active rearrangement of single atoms [6, 10]. An alternative approach is to use the Mott insulator transition to initialize a three-dimensional register by loading a Bose-Einstein condensate into an optical lattice [11]. Recent progress has shown subwavelength addressability in such a system [12]. To perform quantum computations, however, an additional key feature is the ability to perform the gate between two arbitrary qubits of the register.

Here we demonstrate a scheme where a neutral atom qubit is transfered between two moving tweezers ("register" to "moving head"), and then transported towards an interaction zone where the two-qubit gate should be implemented [13, 14, 15, 16]. We show that these manipulations of the external degrees of freedom preserve the coherence of the qubit, and do not induce any heating. This transport in a moving tweezer is a promising alternative to the recently demonstrated transport of qubits in "optical conveyor belts" [6, 17], or in state-dependent moving optical lattices [18]. Altogether, these results

pave the way towards a scalable neutral atom quantum computing architecture.

In our experiment, we trap a single rubidium 87 atom in an optical dipole trap created by a tightly focused laser beam [19, 20]. As described in detail in [21], the qubit is encoded onto the $|0\rangle = |F = 1, M = 0\rangle$ and $|1\rangle = |F = 2, M = 0\rangle$ hyperfine ground states separated by $\omega_{\rm hf} \approx 6.8$ GHz. We initialize the qubit in state $|0\rangle$ by optically pumping the atom. We drive single-qubit operations by a Raman transition using two phased-locked laser beams, one of which being the dipole trap. The internal dephasing time of the qubit, measured by Ramsey interferometry, is ≈ 630 μsec. This time is mostly limited by the residual motion of the atom in the trap that leads to a fluctuation of the frequency of the qubit transition. This dephasing can be reversed by applying a spin echo technique where a π pulse is inserted between the two $\pi/2$ pulses of the Ramsey sequence. Using this technique we measure an irreversible dephasing time of 34 ms.

The experimental setup for the moving tweezer is represented in figure 1. We reflect the dipole trap beam off a mirror affixed to a tip-tilt platform prior to the large numerical aperture lens. The platform is actuated by piezo-electrical transducers and can rotate with a maximal angle of 2.5 mrad in both the horizontal and vertical directions. We have measured the position of the dipole trap for different angles of the platform by observing the position of the atom on the CCD camera. The maximal angle corresponds to a total displacement of the tweezer of 18 ± 1 μm. This motion is two-dimensional, as demonstrated in figure 1.

We first analyze the influence of a displacement of the tweezer on the external degrees of freedom of the qubit. For this purpose, we measure the temperature of the single atom in the tweezer using a release and recapture technique [22] (see Methods). In the absence of motion, the temperature of the atom is 56.0 ± 1.4 μK. We repeat this measurement after moving the tweezer by a total distance of 360 μm, consisting of 20 round trips of 18 μm, along the z-axis. Each round trip lasts a time of 6 ms. We do not find any measurable loss due to this transport. After the motion, we measure a temperature of 54.8 ± 1.6 μK. As the energy difference between two vibrational quanta in the radial direction is 4 μK, this temperature is compatible with no change in the radial vibrational state. This absence of motional heating is a crucial feature for entanglement schemes based on controlled collisions [16, 23] and results from the adiabaticity of the displacement. A motion is adiabatic if the
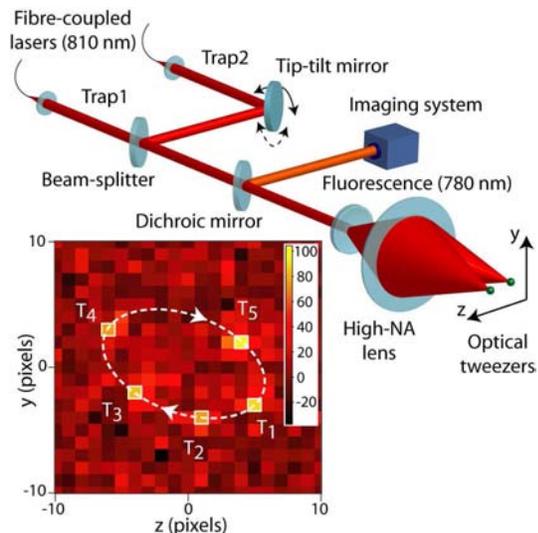
FIG. 1: Experimental setup. A large numerical aperture lens focuses two independent dipole trap beams at 810 nm each to a size of 0.9 micrometers. An optical power of 400 μW results into a trap depth of 500 μK and oscillation frequencies of 81 kHz and 15 kHz, in the radial and axial directions respectively. The two trapping lasers have the same linear polarization and their frequencies are separated by 10 MHz to avoid interferences. The moving tweezer is displaced by rotating a tip-tilt platform. The same large numerical aperture lens is used to collect the fluorescence light at 780 nm from the atom. This fluorescence light is separated from the trapping light by the dichroic mirror and sent to a single-photon counter module and a CCD camera. The insert shows a fluorescence picture of an atom moved along an elliptical trajectory in the y-z plane. The picture is a summation of 5 images taken at different times during the motion.

acceleration a fulfills $ma\sigma \ll \hbar\Omega$ (Ω is the oscillation frequency of the atom, m its mass and σ the extension of the ground state wave function [24]). This gives a maximum acceleration of $\approx 10^4$ m/sec^2, much larger than the experimentally measured ≈ 15 m/sec^2.

We secondly study the influence of the motion on the coherence of the qubit. As the duration of the transport is larger than the dephasing time of the qubit (630 μs), we apply the spin echo sequence to rephase the qubit [21]. The time sequence of the experiment is shown in figure 2. Figure 3(a) shows the amplitude of the spin-echo fringes for various trap displacements along the y-axis. This amplitude is constant when we scan the tweezer over all the transverse field of the objective. This demonstrates that the motion does not affect the internal coherence of the qubit. We observe the same behavior when we move the tweezer along the z-axis.

We also observe a phase shift of the spin-echo fringes, as shown in figure 3(b). This is a signature that the two states of the qubit dephase with respect to each other during the motion (in a reproducible way), despite the presence of the rephasing π pulse. We attribute this phase shift to the asymmetry of the trajectory during
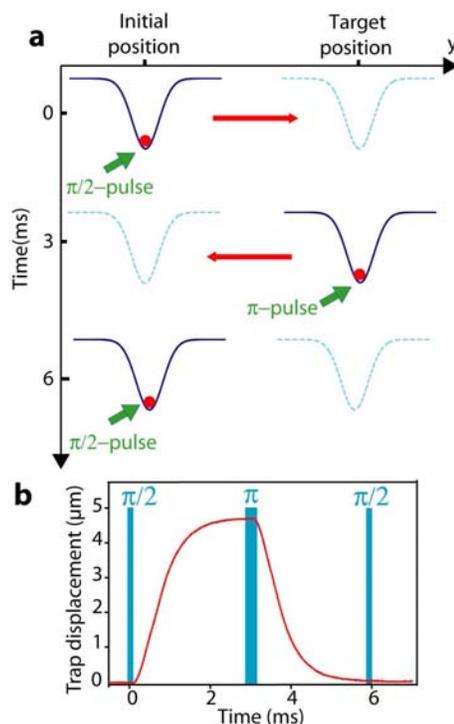

FIG. 2: Principle of the moving qubit experiment. (a) Position of the atom when the pulses of the spin echo sequence are applied. Starting at the initial position, the first pulse prepares the atom in a superposition $(|0\rangle + |1\rangle)/\sqrt{2}$. The tweezer is then moved along the y-axis to the target position and the π pulse is applied. Finally, the tweezer is brought back to its initial position and the coherence is checked by applying a second $\pi/2$ pulse and measuring the state of the qubit. (b) Example of displacement of the tweezer versus time. The signal is obtained from the sensor attached to the tip-tilt platform, which is converted into a distance travelled by the tweezer. The $\pi/2$ and π pulses, being 2 and 4 μs long respectively, are not to scale.

the first and second part of the round trip displacement. We have modelled this effect and found a good agreement with the data (see Methods section). This understanding of the phase evolution of the qubit during the motion is crucial for a possible implementation in a quantum computer where qubit phases need to be controlled.

With the idea of transfering an atom from the "register" to the "moving head", we have investigated the transfer of a qubit from one tweezer to a second one. For this experiment, the two traps are superimposed and the positions of both tweezers are fixed. The experimental sequence is shown in figure 4(a). We load an atom in the first tweezer, transfer it to a second tweezer, and transfer it back to the first tweezer, with no measurable loss. When the two traps have the same depth, we measure a temperature of the atom after the double transfer of 56.3 ± 1.8 μK, while the temperature with no transfer is 53.4 ± 1.4 μK. Therefore, the transfer does not induce any significant motional heating.
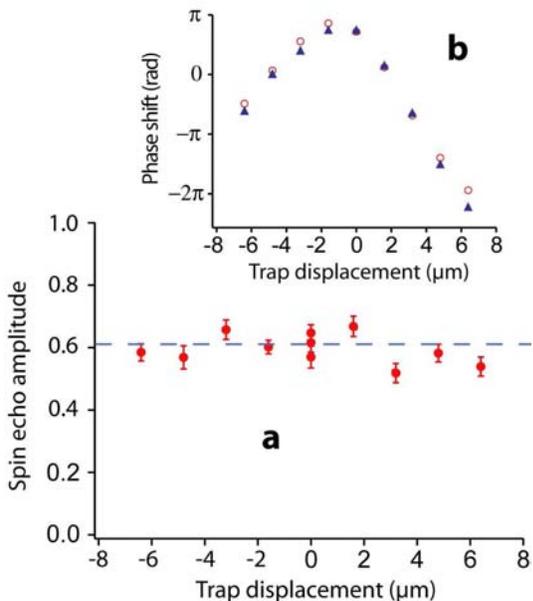
FIG. 3: Results of the moving qubit experiment. Figure (a) shows the amplitude of the spin echo signal versus the amplitude of the displacement. The error bars are the root mean square (RMS) uncertainty obtained from the fit of the fringes. The 60% contrast is a result of the damping of the fringes after 6 ms [21]. The dashed line represents the average of the data for no trap displacement. Figure (b) shows the phase shift versus the amplitude of the displacement. The triangles are the data and the circles are the calculated value of the dephasing based on the model described in the Methods section.

We analyze the influence of the transfer on the coherence of the qubit by inserting the double transfer between the two $\pi/2$ pulses of a Ramsey sequence, as shown in figure 4(a). Figure 4 presents the amplitude and the phase of the Ramsey fringes after this sequence for depths of the second tweezer ranging from 0.2 mK to 0.6 mK. This transfer does not affect the amplitude of the Ramsey signal when the depth of the second trap is varied, thus showing that the coherence is robust against the transfer between the two traps.

Figure 4(c) shows that the phase of the Ramsey fringes, varies linearly with respect to the depth of the second trap. This is explained by the differential potential experienced by the two states, which is proportional to the depth of the trap U. If the depths of the two traps differ by ΔU, the Ramsey fringes are shifted after a holding time T by a phase proportional to $\Delta U \, T/\hbar$, with respect to the situation where no transfer is applied. This phase is thus a useful tool to make sure that the two traps are identical.

As a conclusion we have shown that we can move and transfer a single qubit between two tweezers with no measurable motional heating. We have also shown no loss of coherence of the atomic qubit under transfer and displacement. In combination with our holographic array of
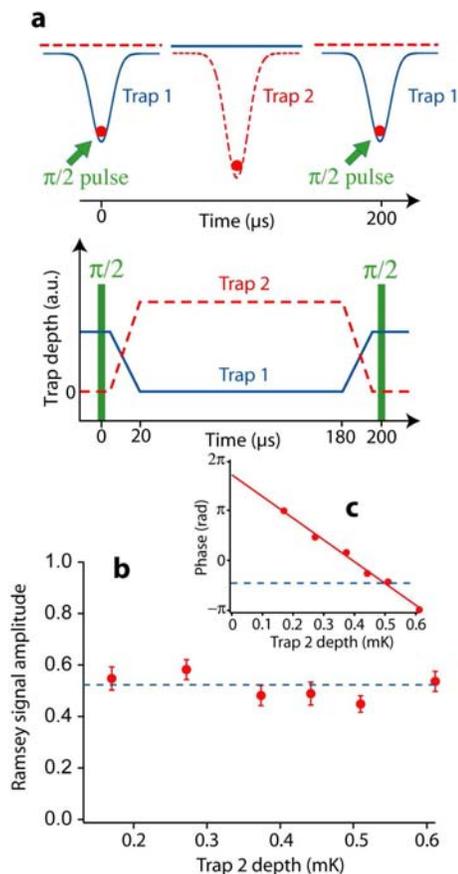

FIG. 4: Experiment on the transfer of the qubit between two tweezers. Figure (a) details the time sequence. A $\pi/2$ pulse is applied when the atom is initially in trap 1, which has a depth of 500 μK. The atom is transferred to trap 2 in a time of 20 μs. After a time of 160 μs, the atom is transferred back to trap 1 and a second $\pi/2$ pulse is applied. Figure (b) shows the amplitude of the spin echo signal as a function of the depth of the trap the atom is transferred into. The error bars are the RMS uncertainty obtained from the fit of the fringes. Figure (c) displays the phase of the Ramsey oscillations for different depths of the second trap. The solid line is a linear fit to the data. The dashed lines in (b) and (c) correspond to no transfer.

dipole traps [4], and efficient single-qubit operation and readout [21], we have made a first step towards designing a scalable architecture of a quantum computer based on neutral atoms.

Methods:

Temperature measurement:

After trapping a single atom, we switch off the dipole trap for a time adjustable between 1 and ~ 30 μsec. We then turn the trap back on and check for the presence of the atom. We repeat this sequence 100 times for each release time and calculate the probability to recapture the atom after the corresponding time of flight. We compare

our data with a 3-dimensional Monte Carlo simulation, taking into account the potential produced by the Gaussian trapping beam, and assuming a thermal distribution of the position and the velocity of the atom at the beginning of the time of flight. The error bar of this fitted temperature corresponds to one standard deviation in the least square-based fit.

Phase shift during the motion:

The hyperfine splitting of 6.8 GHz means that the dipole trap detuning is slightly larger for $|0\rangle$ than for $|1\rangle$, giving rise to a small differential lightshift. Therefore the qubit transition frequency is $\omega_{\mathrm{hf}} + \eta U/\hbar$, with U the depth of the dipole trap and $\eta = 7 \times 10^{-4}$ for our trap. If the tweezer is not moved, the π-pulse compensates for the phase accumulated during the two parts of the motion. When the tweezer is moved off axis, the waist of the beam increases sligthly, resulting in a shallower trap. Figure 2(a) shows that with the tweezer starting on axis, the atom spends more time far from the axis where the dipole trap is shallower, whereas on the way back it spends more time around the axis where the dipole trap is stronger. The average depth is then different for the two parts of the motion, and so are the phases. As the phase of the spin-echo signal is the difference of the phases accumulated during the two periods of the motion, it is expected to vary as we move the tweezer further away off axis. We have modelled this effect by calculating the dephasing accumulated during the transport, taking into account the actual displacement of the tweezer from the sensor curve and the measured Rabi frequencies for different positions of the tweezer off axis. The result of this model is shown as circles in figure 3(b) and is consistent with the data.

[1] Nielsen, M.A., & Chuang, I.L. *Quantum Computation and Quantum Information.* Cambridge University Press (2000)

[2] Kielpinski, D. , Monroe, C., & Wineland, D.J. Architecture for a large-scale ion-trap quantum computer. *Nature* **417**, 709 (2002)

[3] Calarco, T., Dorner, U., Julienne, P.S., Williams, C.J., & Zoller, P. Quantum computations with atoms in optical lattices: Marker qubits and molecular interactions. *Phys. Rev. A* **70**, 012306 (2004)

[4] Bergamini, S. *et al.*, Holographic generation of microtrap arrays for single atoms using a programmable phase modulator. *J. Opt. Soc. Am. B* **21** 1889, (2004).

[5] Dumke, R., *et al.* Micro-optical Realization of Arrays of Selectively Addressable Dipole Traps: A Scalable Configuration for Quantum Computation with Atomic Qubits. *Phys. Rev. Lett.* **89**, 097903 (2002)

[6] Miroshnychenko, Y. *et al.* Quantum engineering: An atom-sorting machine. *Nature* **442**, 151 (2006)

[7] Chiaverini, J., et al. Implementation of the semiclassical quantum Fourier transform in a scalable system. *Science* **308**, 997 (2005)

[8] Seidelin S. *et al.* Microfabricated Surface-Electrode Ion Trap for Scalable Quantum Information Processing *Phys. Rev. Lett.* **96**, 253003 (2006)

[9] Rowe, M.A., *et al.* Transport of quantum states and separation of ions in a dual RF ion trap. *Quantum Information and Computation* **2**, 257-271 (2002)

[10] Schrader, D., *et al* Neutral Atom Quantum Register, *Phys. Rev. Lett.* **93**, 150501 (2004)

[11] Greiner, M., Mandel, O., Esslinger, T., Haensch, T.W., & Bloch, I., Quantum phase transition from a superfluid to a Mott insulator in a gas of ultracold atoms. *Nature* **415**, 39 (2002)

[12] Lee, P. J., *et al.* Subwavelength addressability and spin-dependent transport in a double-well optical lattice. arXiv:quant-ph/0702039

[13] Jaksch, D., Briegel, H.J., Cirac, J.I., Gardiner, C.W. & Zoller, P. Entanglement of Atoms via Cold Controlled Collisions. *Phys. Rev. Lett.* **82** 1975 (1999)

[14] Brennen, G.K., Caves, C.M., Jessen, P.S., & Deutsch, I.H. Quantum Logic Gates in Optical Lattices. *Phys. Rev. Lett.* **82**, 1060 (1999)

[15] Jaksch, D., *et al.* Fast Quantum Gates for Neutral Atoms. *Phys. Rev. Lett.* **85** 2208 (2000)

[16] Dorner U., Calarco T., Zoller P. Browaeys A. & Grangier P. Quantum logic via optimal control in holographic dipole traps *J. Opt. B: Quantum Semiclass. Opt.* **7**, S341 (2005)

[17] Kuhr, S., *et al.* Coherence Properties and Quantum State Transportation in an Optical Conveyor Belt. *Phys. Rev. Lett.* **91**, 213002 (2003)

[18] Mandel, O., *et al.* Coherent Transport of Neutral Atoms in Spin-Dependent Optical Lattice Potentials. *Phys. Rev. Lett.* **91**, 010407 (2003).

[19] Schlosser, N., Reymond, G., & Grangier, P., Collisional Blockade in Microscopic Optical Dipole Traps. *Phys. Rev. Lett.* **89**, 023005 (2002).

[20] Sortais, Y.R.P., *et al.*, Diffraction-limited optics for single-atom manipulation. *Phys. Rev. A* **75**, 013406 (2007).

[21] Jones, M.P.A., *et al.* Fast quantum state control of a single trapped neutral atom. *Phys. Rev. A* **75**, 040301(R) (2007)

[22] Lett, P., *et al.* Observation of Atoms Laser Cooled below the Doppler Limit. *Phys. Rev. Lett.* **61** 169 (1988)

[23] Mandel O., *et al.* Controlled collisions for multi-particle entanglement of optically trapped atoms. *Nature* **425**, 937 (2003)

[24] Browaeys, A., *et al.* Transport of atoms in a quantum conveyor belt. *Phys. Rev. A* **72**, 053605 (2006)